SRM COMBUSTION STABILITY WITH TWO-PHASE FLOW EFFECTS

Toru SHIMADA

Japan Aerospace Exploration Agency

ABSTRACT

Quasi-one-dimensional gas-particle fluid dynamics in combustion chamber, local thermal conduction within solid propellant, and quasi-steady flame model over propellant surface are simultaneously solved to predict linear acoustic stability characteristics of metallized solid propellant combustion in a motor-nozzle system. Simulation results, compared with a linear theory, show good agreement except at high particle diameters for heavily loaded conditions, where gas-particle equilibrium assumption breaks. Effects of realistic drag and heat transfer model are also discussed.

INTRODUCTION

The oscillatory combustion of solid rocket motor (SRM) is classified into the acoustic combustion instability and the non-acoustic instability. The acoustic combustion instability, which is caused by the resonance between the natural acoustic oscillation of the flow and the fluctuation of the propellant burning rate in the combustion chamber, can cause blowup of combustion chamber.

The theoretical analysis of the combustion instability is divided into linear analyses and nonlinear analyses. A linear analysis is usually based on a small perturbation method and the application of the theory is limited to cases of small amplitude oscillations. On the other hand, a nonlinear analysis is done for a finite amplitude oscillation. Although many recent researches handle nonlinear problems, the linear analysis is also important because a nonlinear phenomenon is often a result of amplification of minute acoustic oscillations.

In the past decades, ability of computational technologies has improved greatly. Researches on the combustion instability of SRM are heading for advanced simulations of multidimensional, turbulent, and multiphase flows. Recently, the author's group has demonstrated both quasi-one-dimensional (Q1D) and axisymmetric non-steady analyses on combustion stability of solid rocket motor by combining CFD flow calculation, thermal conduction within propellant, and a quasi-steady flame model [1]. Linear and non-linear problems [2] have been analyzed by this methodology so far.

In this report, the previous technique is extended to two-phase flow of aluminized solid-propellant rocket motor. Growth rate of a small fluctuation is evaluated and compared with theoretical values. In the following part of the paper, firstly the mathematical model is described, and then the numerical results will be shown. Discussion will be made on the growth rates versus the particle diameter for representative values of the loading ratio, the heat release in the surface reaction, and the activation energy.

METHOD OF ANALYSIS

Solid Rocket Motor Configuration

Combustion gas in SRM is modeled as a mixture of a gas phase and a particle phase. The particle phase is a representative of molten-liquid droplets of aluminium and alumina. Although in reality particles of various diameters coexist in combustion gas, in the present modelling particles are assumed to have one common diameter, which is treated as one of computational parameters.

It is known that two kinds of speed of sound can be defined at the limits of the Stokes number S_t in multiphase flow dynamics. A Stokes number is usually the ratio of a relaxation time of the velocity or the temperature between the two-phases to those of gas to a representative time scale of gas flow. When

particle diameter is sufficiently small, the Stokes number approaches zero. At the limit of $S_t \to 0$, the speed of sound is defined by the equilibrium value. On the other hand, when the Stokes number is very large, the speed of sound reaches the frozen value. The equilibrium speed of sound a_e in a gas with dispersed particles can be given by the following expression,

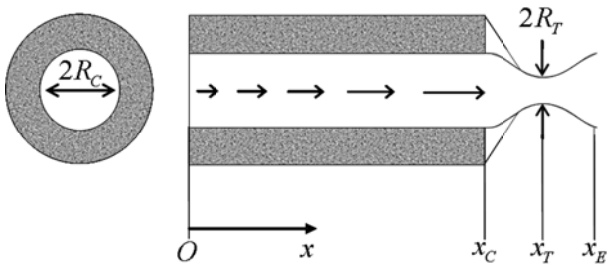

Figure 1. Configuration of Solid Rocket Motor.

$$a_e = \sqrt{\frac{c_p + \psi c}{c_v + \psi c}\frac{p}{(1+\psi)\rho_g}}, \tag{1}$$

where c_p and c_v are specific heats at constant pressure and at constant volume, respectively, c is specific heat of particle material, ψ is the loading ratio, p is the pressure, and ρ_g is the gas density.

Let us consider a domain of computation, $0 \le x \le x_E$, where x_E is the location of the nozzle exit as shown in Figure 1. The combustion chamber lies in $0 \le x \le x_C$, ($x_C < x_E$) and a Laval nozzle is connected to the chamber at x_C. The nozzle extends from x_C to x_E with the throat at $x = x_T$. The length of the nozzle is defined as $x_E = 1.05x_C$ in order not to conflict with applicability of the short nozzle theory [3] which we will use to evaluate the acoustic attenuation at the nozzle entrance. The x_C is set to the value that the frequency of the first axial mode of acoustic oscillation is close to the resonance frequency f_r of the solid propellant combustion as,

$$f_r = \frac{a_e}{2x_C}, \tag{2}$$

where a_e is defined by Eq. (1). The resonance frequency is found as the value at which the pressure perturbation response has local maximum. In the present study we set f_r =131Hz for the set of parameters used.

The radius of the port cross section at x is defined as

$$r_C(x) = \begin{cases} R_C & \text{for } 0 \le x \le x_C \\ R_T - \dfrac{(R_C - R_T)}{(x_C - x_T)^4}(x - x_T)^4 + \dfrac{2(R_C - R_T)}{(x_C - x_T)^2}(x - x_T)^2 & \text{for } x_C \le x \le x_E \end{cases} \tag{3}$$

where R_T is the throat radius, R_C is the combustion chamber port radius and, at the same time, the radius of the propellant burning surface in this study. Both R_C and R_T do not change with the time. The values of R_C and R_T are determined by the similar method described in the previous study [1]. The only difference in the present study is that we employ the equilibrium values for the Mach number and the specific heat ratio, and the gas constant. The nozzle entrance Mach number M_N is defined by $M_N = (u/a_e)_N$.

Basic Equations for Fluid Dynamics in the Combustion Chamber and the Nozzle

The governing equations for Q1D unsteady gas-particle flow with mass addition and gas-particle two-way coupling are written. In a quasi-one-dimensional formulation, the effect of the axial change of the contour of the motor chamber and the nozzle appears in the first source term and for the present case as those including dr_C/dx. The mass addition from the burning surface appears in the second source term as a result of integration over the perimeter boundary of the propellant grain surface. Similar approach has been used and reported in literature [4]. The gas-particle two-way coupling interaction appears in the third source term, in which the momentum and the energy coupling are considered.

$$\frac{\partial \boldsymbol{q}}{\partial t}+\frac{\partial \boldsymbol{f}}{\partial x}=\boldsymbol{S}_{q1d}+\boldsymbol{S}_{ma}+\boldsymbol{S}_{gpi} \tag{4}$$

$$\boldsymbol{q}=\begin{bmatrix}\rho\\ \rho u\\ \rho\varepsilon\\ \rho_p\\ \rho_p u_p\\ \rho_p\varepsilon_p\end{bmatrix},\quad \boldsymbol{f}=\begin{bmatrix}\rho u\\ \rho u^2+p\\ \rho uH\\ \rho_p u_p\\ \rho_p u_p^2\\ \rho_p u_p\varepsilon_p\end{bmatrix},\quad \boldsymbol{S}_{q1d}=-\frac{2}{r_c}\frac{dr_c}{dx}\begin{bmatrix}\rho u\\ \rho u^2\\ \rho uH\\ \rho_p u_p\\ \rho_p u_p^2\\ \rho_p u_p\varepsilon_p\end{bmatrix},\quad \boldsymbol{S}_{ma}=\frac{2}{r_c}\begin{bmatrix}m_b\\ 0\\ m_b c_p T_f\\ m_{bp}\\ 0\\ m_{bp}cT_f\end{bmatrix},\quad \boldsymbol{S}_{gpi}=\begin{bmatrix}0\\ -\Gamma_{mo}\\ -\Gamma_{ec}-\Gamma_{mo}u_p\\ 0\\ \Gamma_{mo}\\ \Gamma_{ec}+\Gamma_{mo}u_p\end{bmatrix} \tag{5}$$

where t and x are the time and the space, respectively and $r_C(x)$ is the radius of the port cross section at x. As for the gas phase, ρ is the density, u the velocity, ε the specific total energy, p the pressure, H the total enthalpy, and c_p the specific heat of at constant pressure. As for the particle phase, ρ_p is the bulk density, u_p the velocity, ε_p the specific total energy, and c the specific heat. The flame temperature T_f is assumed to be common between the phases. The mass addition rates per unit surface area for gas phase and particle phase, respectively, are defined as

$$m_b=(1-\phi)\rho_s\dot{r}_b,\qquad m_{bp}=\phi\rho_s\dot{r}_b, \tag{6}$$

where ρ_s is the density of propellant, $\dot{r}_b$ is the linear burning rate, and ϕ is the mass fraction of alumina in combustion gas.

Thermodynamic properties of gas, particle, and propellant are assumed to be constant for simplicity. The equation of state for gas is $p=\rho RT_g$. The specific total energies for the two phases are given by the following, respectively,

$$\varepsilon=\frac{1}{\gamma-1}\frac{p}{\rho}+\frac{1}{2}u^2,\qquad \varepsilon_p=cT_p+\frac{1}{2}u_p^2 \tag{7}$$

where γ is the specific heat ratio, R the gas constant, and T_g the gas temperature.

The momentum exchange between phases can be written as

$$\Gamma_{mo} = \frac{3}{4}\frac{\rho\rho_p}{\sigma_m}\left|u-u_p\right|C_D\frac{1}{d_p}\left(u-u_p\right) = \frac{\rho_p}{\tau_V}\left(u-u_p\right) \tag{8}$$

where σ_m is the true density of the particle, d_p is the particle diameter, C_D is the drag coefficient, and τ_V is a relaxation time for velocity and defined by

$$\tau_V \equiv \frac{4}{3}\frac{\sigma_m}{\rho}\frac{d_p}{C_D\left|u-u_p\right|} = \frac{4}{3}\frac{1}{\mathrm{Re}_r}\frac{\sigma_m d_p^2}{\mu C_D}, \tag{9}$$

where Re_r is the particle Reynolds number based on the relative speed $\left|u-u_p\right|$, μ the viscosity coefficient.

The energy exchange between phases can be written as

$$\Gamma_{ec} = 6\frac{\mathrm{Nu}}{\mathrm{Pr}}\frac{1}{d_p^2}\frac{\rho_p}{\sigma_m}\mu c_p\left(T-T_p\right) = \frac{\rho_p c}{\tau_T}\left(T-T_p\right), \tag{10}$$

where Nu is the Nusselt number, Pr is the Prandtl number, and τ_T is a relaxation time for temperature and defined by

$$\tau_T \equiv \frac{1}{6}\frac{\mathrm{Pr}}{\mathrm{Nu}}\frac{\sigma_m d_p^2}{\mu}\frac{c}{c_p}. \tag{11}$$

Initial and Boundary Conditions

The initial condition is defined as

$$\boldsymbol{q}\left(x,0\right) = \boldsymbol{q}_0\left(x\right) + \boldsymbol{q}'\left(x\right). \tag{12}$$

The first term in the right-hand side is the conserved-value vector at the steady state. The second term in the right-hand side of Eq. (12) is a small perturbation vector. It is defined by superimposing the first mode standing pressure wave to the steady-state pressure field as

$$p\left(x,0\right) = p_0\left(x\right) - p'\cos\left(\frac{\pi x}{x_C}\right), \tag{13}$$

where the amplitude p' is set to 0.1% of the combustion pressure p_c.

The boundary conditions at $x=0$ are for the specularly-reflecting wall imposed assuming that there is an inert wall at the head end, i.e.,

$$\frac{\partial\rho\left(0,t\right)}{\partial x} = \frac{\partial p\left(0,t\right)}{\partial x} = u\left(0,t\right) = 0, \qquad \frac{\partial\rho_p\left(0,t\right)}{\partial x} = \frac{\partial T_p\left(0,t\right)}{\partial x} = u_p\left(0,t\right) = 0, \tag{14}$$

and the supersonic outflow condition is imposed at $x = x_E$. The outflow condition is unsteadily imposed in the numerical simulation, namely, the instantaneous inner-region quantities are extrapolated to the outer ghost cell.

Basic Equation for Thermal Conduction in the Solid Propellant

Let us assume, at each station of $x \le x_C$, a semi-infinite, homogeneous solid propellant to burn in a one-dimensional manner to the negative direction of y-axis, the local coordinate system always fixed to the burning surface. The unsteady heat conduction in the solid propellant is described by the one-dimensional unsteady heat conduction equation.

$$\frac{\partial T}{\partial t} + \dot{r}_b \frac{\partial T}{\partial y} - \alpha_s \frac{\partial^2 T}{\partial y^2} = 0, \quad t \ge 0, \quad -\infty \le y \le 0 \tag{15}$$

where $T = T(y,t)$ is the temperature of the solid propellant, α_s is the thermal diffusivity defined by

$$\alpha_s = \lambda_s / (\rho_s c_s), \tag{16}$$

with λ_s the thermal conductivity and c_s the specific heat.

The initial condition for the thermal equation is defined by the steady-sate solution

$$T(y,0) = \overline{T}(y) = T_a + (T_{S0} - T_a)\exp\left(\frac{\dot{r}_{b0}}{\alpha_s} y\right) \tag{17}$$

for the boundary condition

$$\overline{T}(0) = T_{S0}, \quad \overline{T}(-\infty) = T_a, \tag{18}$$

where T_a is the initial temperature of the solid propellant.

The boundary conditions for the thermal conduction equation are defined as

$$T(-\infty,t) = T_a, \quad T(0,t) = T_S(t), \tag{19}$$

$$\lambda_s \left.\frac{\partial T(y,t)}{\partial y}\right|_{y=-0} = \lambda_g \left.\frac{\partial T(y,t)}{\partial y}\right|_{y=+0} + \rho_s \dot{r}_b(t) Q_S \tag{20}$$

where the surface temperature $T_S(t)$ is unknown value which must be determined at each moment through the simultaneous solution of the fluid dynamics and the thermal conduction. The thermal conduction coefficient of the gas is denoted by λ_g and the heat release due to the surface reaction per unit mass of the generated gas by Q_S.

Quasi-Steady Flame Model

Let us consider the one dimensional combustion region and assume it to be divided into a heating zone in the solid ($y < 0$), an exothermic reaction surface ($y = 0$), and a gaseous reaction zone ($0 < y \le \delta$) as shown in Figure 2. There have been studied by many researchers on the flame models and reviews on this topic are available [5], [6]. The flame model employed here was first proposed by Hanzawa in 1976 for the theoretical study on depressurization induced extinction of solid propellant [7], [8].

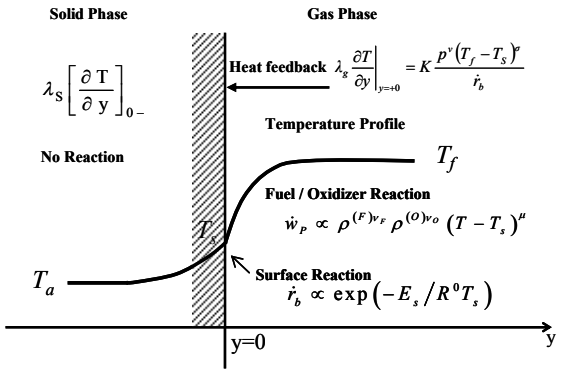

Figure 2. Quasi-steady flame model.

Within the flame layer of the thickness δ , which is considered very small, the non-constant gaseous reaction is considered and the solution is integrated over the thickness to get the heat feedback amount to the burning surface. It is also assumed that the reaction occurs through an irreversible pyrolysis process and the gas phase reaction through a one step-forward type overall process between gaseous fuel and oxidizer.

In this study the stoichiometric mixture of the oxidizer and the fuel is considered. The Lewis number of the gas mixture is taken as unity. Furthermore in the flame zone ($0 \le y \le \delta$) the gas phase processes are assumed to be quasi-steady since the relaxation times of the processes are much smaller than those of the solid propellant thermal conduction and the gas-dynamics in the chamber. Detailed description was given in the previous report [1].

In this model, the amount of the heat feedback, i.e., the right(+)-side temperature gradient at the burning surface, can be expressed as follows,

$$\lambda_g \left.\frac{\partial T}{\partial y}\right|_{y=+0} = K \frac{p^{\nu}\left(T_f - T_S\right)^{\sigma}}{\dot{r}_b}, \quad \sigma = \nu + \mu + 1, \quad \nu = \nu^{(F)} + \nu^{(O)} \tag{21}$$

where K is a constant. This heat feedback law was derived based on a distributed gas phase reaction [7], [8]. The case of a large value of σ represents a sharp flame or flame sheet, whereas the case $\sigma = 1$ corresponds to a uniform distribution of reaction rate. Although the latter heat feedback law was first employed by Akiba and Tanno [9] to elucidate L* combustion instability, Krier, T'ien, Sirignano, and Summerfield [10] derived it theoretically for composite propellants. Thus, it is often called a KTSS model. The above heat feedback law accommodates both cases. It has been demonstrated in the previous papers [1], [2] that this heat-feedback expression is useful for the fully-coupled linear and non-linear oscillatory combustion fluid-dynamic computation.

By solving the coupled system of the fluid dynamics and the thermal conduction, the surface temperature $T_S(t)$ at each time is obtained. The linear burning rate is then obtained from an Arrhenius-type function of the surface temperature: $\dot{r}_b(t) = \dot{r}_{b0} \exp\left[-\left(E_s/R^0\right)\left(1/T_S(t) - 1/T_{S0}\right)\right]$.

Numerical Procedure

It has been demonstrated that a conventional Finite-Volume Method (FVM) with second-order MUSCL approach can provide a sufficient precision for the prediction of small perturbation growth or decay [1]. In the present simulation, FVM with third-order MUSCL space discretization with the 2nd-order TVD Runge-

Kutta time integration is employed. Whereas in the previous paper, the local Lax-Friedrich scheme was used to evaluate the numerical convective flux, Simple Low-dissipative AUSM (SLAU) scheme [11] is used. The usage of this scheme is because of its low dissipative characteristics at low speeds, which seems to be good for our current purpose. As for the thermal conduction in the solid propellant, the basic equation is nondimensionalized and converted through an exponential transformation, and then discretized by the second-order finite difference method. Detailed description was given in the previous paper.

THEORETICAL EVALUATION

Linear Growth Rate of the First Acoustic Mode

As the results of the linear theory [12], the growth rate of the first acoustic mode for the present gas-particle flow situation can be written as

$$\alpha = \alpha_C + \alpha_N + \alpha_{Ft} + \alpha_P$$

$$\alpha_C = \frac{a_{e0}\overline{\gamma}}{R_C} R_p^{(r)} M_{b0} = \frac{a_{e0}\overline{\gamma}}{2x_C} R_p^{(r)} M_{N0}, \quad \alpha_N = -\frac{a_{e0}}{x_C}\left(\frac{\overline{\gamma}+1}{2}\right) M_{N0}, \quad , \tag{22}$$

$$\alpha_{FT} = -\frac{a_{e0}}{R_C} M_{b0} = -\frac{a_{e0}}{2x_C} M_{N0}, \qquad \alpha_P = -\frac{\omega_1}{2}\frac{\psi}{1+\psi}\left[\frac{\Omega_d}{1+\Omega_d^2} + (\overline{\gamma}-1)\frac{C}{\overline{C}_p}\frac{\Omega_t}{1+\Omega_t^2}\right]$$

where $R_p^{(r)}$ is the real part of the response function defined by the following equation [13],[14]

$$R_p \equiv \frac{\dot{r}_b'/\dot{r}_{b0}}{p'/p_0} = \frac{nAB}{\lambda + \frac{A}{\lambda} - (1+A) + AB}. \tag{23}$$

Standard definitions of *A*, *B*, *n*, and λ are used as given in [1]. The definitions of the parameters in the expression of α_P are given in [12] and summarized as follows.

$$\omega_1 = 2\pi f_1, \quad \Omega_d = \omega_1 \tau_d, \quad \Omega_t = \omega_1 \tau_t \tag{24}$$

$$\tau_d = \frac{\rho_p d_p^2}{18\mu}, \quad \tau_t = \left(\frac{3}{2}\frac{C\,\mathrm{Pr}}{\overline{C}_P}\right)\tau_d \tag{25}$$

Particles are assumed to be spherical throughout the study. It should be noted that, in the linear theory, the Stokes drag coefficient is used to evaluate the relaxation times, i.e.,

$$C_D = \frac{24}{\mathrm{Re}_r} \tag{26}$$

RESULTS AND DISCUSSION

Growth Rate

The growth rate is evaluated by the same method described in Ref. [1]. The initial perturbation is a cosine wave of the first acoustic mode and its initial amplitude is 0.1% of the chamber pressure p_c. The perturbation is superimposed on the steady-state solution obtained also by the present numerical method. The history of the pressure at the head end of the chamber is utilized to evaluate the growth rate α, i.e.,

$(p_{HE} - p_{0HE})/p_{0HE} \propto \exp[\alpha t]$.

For the present study we employ the values shown in Table 1. Several simulations have been conducted for the sets of combination of Q_S, ψ, and d_p with the nozzle mach number and the activation energy set to 0.2 and 9000 R^0 J/kg, respectively. Simulated cases and results of the growth rate are summarized in Table 2. These results of the growth rate are plotted against the particle diameter and compared with the linear theory for Q_S =548400 J/kg, for 579800 J/kg, and for 600000 J/kg in Figs. 3, 4, and, 5, respectively.

Table 1. Values of Combustion Parameters.

Properties	Value
ν	1.0
σ	4.0
T_a	300 K
T_{S0}	900 K
$\dot{r}_{b0}$	5×10^{-3} m/s
T_{f0}	3500 K
Molecular Weight	18.36 g/mole
c_s, c_p	1381 J-K/kg
α_s	1.5×10^{-7} m^2/s
Q_S	548-600 kJ/kg
E_S/R^0	9000 K

Comparison with the theory shows that the present simulation results agree fairly well for smaller loading ratio and for smaller particle diameters. Discrepancy between them is seen at large particle diameters when the loading ratio is high. The reason of this discrepancy can be attributed to the assumption of the gas-particle equilibrium used in the linear theory. This is understood from the value of the Stokes number plotted in Fig. 6. The Stokes number becomes close to unity for a large diameter and this means non-equilibrium effect becomes significant.

Effect of Realistic Drag and Heat Transfer

In the above simulation, the Stokes drag (Eq.(26)) and limit Nusselt number (Nu=2) are employed to evaluate the relaxation times. It is well known that the Reynolds and Mach number effects become significant as particle diameter becomes large [15]. In order to evaluate the amount of these effects, further simulations have been carried out for Case 2-1 using more realistic models of drag and heat transfer. For the drag coefficient of a sphere, Carlson and Hoglund [16] expression is used with an incompressible drag coefficient of Wen and Yu [17] expression. As for the Nusselt number of a sphere, Kavanau-Drake [18] expression is used. The expressions of these are given also in [15].

Table 2. Summary of Growth Rate Results for Simulation Cases. (Stokes Drag used)

case	M_{N0}	E_S/R^0 K	Q_S J/kg	Metal % ϕ_m (*)	Loading Ratio ψ (*)	Growth Rate, 1/s d_p, μm				
						6	12	24	48	96
1-1	0.2	9000	548400	20	≈0.6	-35.77	-62.92	-138.39	-172.97	-90.99
1-2	0.2	9000	↑	5	≈0.1	-26.38	-32.57	-49.02	-41.90	-29.70
1-3	0.2	9000	↑	0.5	≈0.01	-21.47	-22.34	-23.25	-22.43	-21.41
2-1	0.2	9000	579800	20	≈0.6	-10.96	-36.97	-99.16	-146.86	-70.83
2-2	0.2	9000	↑	5	≈0.1	-5.21	-7.88	-21.34	-14.40	-6.52
2-3	0.2	9000	↑	0.5	≈0.01	2.27	1.11	0.01	0.37	1.87
3-1	0.2	9000	600000	20	≈0.6	18.86	-2.01	-55.46	-84.71	-45.88
3-2	0.2	9000	↑	5	≈0.1	33.11	22.56	11.76	19.45	27.21
3-3	0.2	9000	↑	0.5	≈0.01	32.90	30.08	29.29	29.81	32.91

(*) $\psi = \dfrac{\rho_p}{\rho} = \dfrac{\phi}{1-\phi}, \qquad \phi = \dfrac{51}{27}\phi_m$

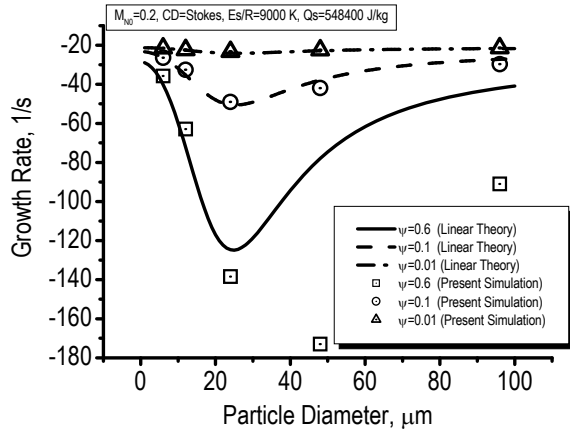

Figure 3 Growth Rate, Comparison with Linear Theory, Cases 1-1, 1-2, and 1-3.

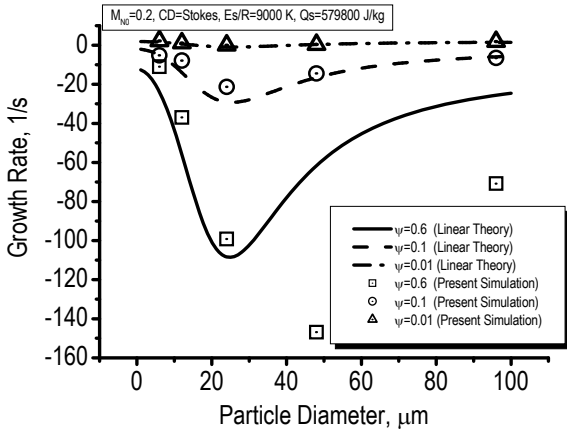

Figure 4 Growth Rate, Comparison with Linear Theory, Cases 2-1, 2-2, and 2-3.

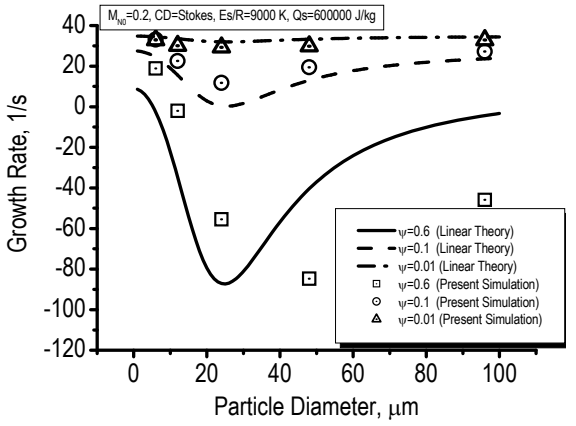

Figure 5 Growth Rate, Comparison with Linear Theory, Cases 3-1, 3-2, and 3-3.

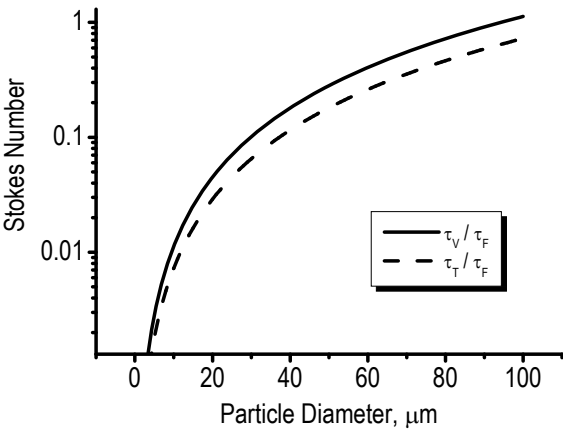

Figure 6 Stokes number vs Particle Diameter

Results of these simulations are shown in Figure 7. It is clear that when more realistic drag and heat transfer coefficients are used, attenuation rate increases in magnitude for large particles, whereas it decreases in magnitude for small particles.

CONCLUSION

We have extended the previously developed mathematical model and numerical schemes for the prediction of the linear stability of solid rocket motor combustion to include gas-particle flow effect. From several simulation results it is confirmed that the present method can provide a good estimation of the decay or the growth of a small perturbation. The present method is directly applicable to non-linear problems and easily extended to multi-dimensional problems.

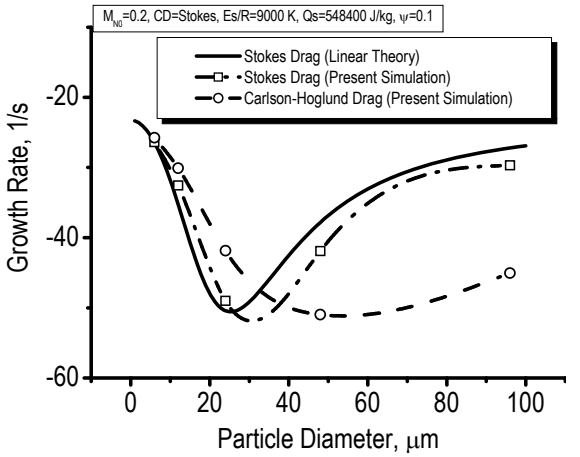

Figure 7 Growth Rate, Effect of realistic drag and heat transfer coefficients. Symbols show present results and are spline interpolated.

ACKNOWLEDGMENTS

This research is supported by JAXA Grant B-UA-09-4K1-UHA18-1009.

REFERENCES

[1] Shimada, T., M. Hanzawa, T. Morita, T. Kato, T. Yoshikawa, and Y. Wada, "Stability Analysis of Solid Rocket Motor Combustion by Computational Fluid Dynamics," AIAA Journal, Vol. 46, No.4, 2008, pp.947-957.

[2] Morita, T., Hanzawa, M., and Shimada, T., "CFD Analyses of Low Frequency Combustion Instability in Solid Propellant Rocket Motors," Advancements in Energetic Materials and Chemical Propulsion, edited by Kenneth K. Kuo and Juan de Dios Rivera, Begell House, Inc., 2007, pp.457-475

[3] Zinn, B., T., "Longitudinal Mode Acoustic Losses in Short Nozzles," Journal of Sound and Vibrations, Vol.22, No.1, 1972, pp. 93-105.

[4] Kooker, D.E., and Zinn, B.T., "Triggering Axial Instabilities in Solid Rockets: Numerical Predictions," AIAA Paper, No.73-1298, AIAA/SAE 9th Propulsion Conference, Las Vegas, Nevada, Nov. 1973.

[5] De Luca, L., "Theory of Nonsteady Burning and Combustion Stability of Solid Propellants by Flame Models," Nonsteady Burning and Combustion Stability of Solid Propellants, Edited by De Luca, L., Price E.W., and Summerfield, M. Progress in Astronautics and Aeronautics, Vol. 143, AIAA, 1992, pp. 519-600.

[6] Jackson, T.L., Massa, L., and Brewster, M.Q., "Unsteady Combustion Modelling of Energetic Solids, Revisited," Combustion Theory and Modelling, Vol. 8, Issue 3, 2004, pp.513-532.

[7] Hanzawa, M., "A Theoretical Study on the Extinction of Solid Propellants by a Rapid Pressure Decay," Doctoral Dissertation, University of Tokyo, 1976.

[8] Hanzawa, M., "A Theoretical Study on Depressurization Induced Extinction of Solid Propellant," AIAA Paper No. 76-635, AIAA/SAE 12th Propulsion Conference, 1976.

[9] Akiba, R. and Tanno, M., "Low Frequency Instability in Solid Propellant Rocket Motors," *Proceedings of the First International Symposium on Rockets and Astronautics*, Tokyo, 1959, pp. 74-82.

[10] Krier, H., T'ien, J.S., Sirignano, W.A., and Summerfield, M., "Non-steady Burning Phenomena of Solid Propellants: Theory and Experiments," *AIAA Journal*, Vol. 6, No. 2, 1968, pp. 278-285.

[11] Shima, E. and Kitammura, K, "On New Simple Low-Dissipation Scheme of AUSM-Family for All Speeds," AIAA Paper 2009-136, 2009

[12] Culick, F.E.C. and Yang, V., "Prediction of Stability of Unsteady Motions in Solid Propellant Rocket Motors," *Nonsteady Burning and Combustion Stability of Solid Propellant*, Progress in Astronautics and Aeronautics, Vol. 143, 1992, pp. 719-804.

[13] Novozhilov, B.V., "Theory of Nonsteady Burning and Combustion Stability of Solid Propellant by the Zeldovich-Novozhilov Method," *Nonsteady Burning and Combustion Stability of Solid Propellant*, Progress in Astronautical and Aeronautics, Volume 143, 1992, pp. 601-641.

[14] Culick, F.E.C., "A Review of Calculations for Unsteady Burning of a Solid Propellant," *AIAA Journal*, Vol. 6, No. 12, 1968, pp.2241-2255.

[15] Shimada, T., Daimon, Y., and Sekino, N., *Computational Fluid Dynamics of Multiphase Flows in Solid Rocket Motors*, JAXA Special Publication JAXA-SP-05-035E, Japan Aerospace Exploration Agency, March 2006.

[16] Carlson D.J. and Hoglund, R.F., "Particle drag and heat transfer in rocket nozzles," *AIAA Journal*, Vol. 2, No. 11, 1964.

[17] Wen, C.Y. and Yu, Y.H., *Chemical Engineering Progress Symposium Series*, Vol. 6, p.100, 1966.

[18] Kavanau, L.L. and Drake, R.M., Jr., "Heat Transfer from Sphere to a Rarefied Gas in Subsonic Flow," Univ. of California, Rept. HE-150-108, p.9, 1953.